

## Time profile of harmonic generation

Carla Figueira de Morisson Faria, Martin Dörr, and Wolfgang Sandner  
*Max-Born-Institut, D-12474 Berlin, Germany*

(Received 20 December 1996)

Information about the time-behavior of high-harmonic generation from a single atom in a strong laser field is obtained through a time-frequency analysis. The solution from the full numerical solution of the time-dependent Schrödinger equation is compared with a widely used two-step semiclassical model of harmonic generation. As a test case, we consider a one-dimensional model “atom” with a short-range potential. The two results are in qualitative agreement only if in the two-step model the initial and final (dipole) interaction matrix elements are suitably chosen. [S1050-2947(97)05605-9]

PACS number(s): 32.80.Rm, 42.65.Ky

The current paradigm of high-harmonic generation in atomic systems involves the physical picture of an electron wave packet being drawn out and away from the atom by the laser field and then driven back hard towards the vicinity of the nucleus, where a strong nonlinear interaction can take place, generating harmonic radiation of the driving fundamental laser frequency. This is the key idea in the two-step semiclassical model [1] in which the emission and return interaction steps are modeled by effective dipole couplings and the semiclassical phase of the intermediate evolution in the field is taken into account. The harmonic response of the atom is always calculated starting from the time-dependent atomic dipole,  $x(t)$ , the absolute magnitude squared of the Fourier transform of the dipole acceleration,  $|\mathcal{FT}[\ddot{x}(t)](\Omega)|^2$ , being proportional to the atomic emission spectrum [2]. To obtain additional temporal information about the production of harmonics, the Fourier transform must be convoluted with a temporally restricted envelope.

Such a time-frequency or “wavelet” analysis has been recently used to analyze the time profile of harmonic emission during a short intense laser pulse [3]. The form of the (Gabor) analyzing wavelet mainly used and also considered here has a Gaussian window and is given by

$$W(t, t_0, \Omega) = \exp[-(t - t_0)^2 / \sigma^2] \exp[i\Omega t]. \quad (1)$$

Usually, the envelope width  $\sigma$  of the wavelet is chosen larger than the laser period  $T = 2\pi/\omega_L$ . The usual Fourier transform, in which all temporal information is lost, is obtained for  $\sigma \rightarrow \infty$ . When investigating harmonic frequencies  $\Omega = N\omega_L$  of the atomic response to the laser, one can, however, choose an envelope even narrower than the fundamental period (as long as  $\sigma > 2\pi/\Omega$ ) [3].

In order to test the validity of the two-step semiclassical model of high-harmonic generation [1,4], we have chosen a test case that is both expedient to solve fully numerically (being one dimensional) and that should be favorable to the application of the two-step approximation. We have thus solved the time-dependent Schrödinger equation for a one-dimensional model “atom” bound by a Gaussian binding potential (in a.u.),  $V(x) = -0.76\exp(-x^2/1.76)$ , which in the absence of the laser supports a single bound state, denoted  $|0\rangle$ , at energy  $E_0 = -0.401$ . This atom is driven by an external field  $\mathcal{E}(t) = -\mathcal{E}_0 \sin(\omega_L t) = -A(t)$  of angular frequency

$\omega_L = 0.05$ , whose amplitude is turned on linearly from 0 to  $\mathcal{E}_0 = 0.08$  over two cycles [5]. The numerical solution is performed in the velocity gauge using standard finite-difference space-grid methods [2].

The two-step model considers only a single bound state of the atom, which is correct for our test case, and it neglects the influence of the atomic potential on the trajectory of the electron driven by the laser field, which again is true as soon as the electron is outside the range of the potential. We have performed a semiclassical calculation similar to [4] for our one-dimensional (1D) case. We computed the time-dependent dipole from the formula [1]

$$x(t) = 2\text{Re} \left\{ \lim_{\epsilon \rightarrow 0} \int_0^{+\infty} d\tau \left( \frac{\pi}{\epsilon + i\tau/2} \right)^{1/2} d_x^* [p_{\text{st}}(t, \tau) - A(t)] \right. \\ \left. \times d_x [p_{\text{st}}(t, \tau) - A(t - \tau)] \mathcal{E}(t - \tau) \exp[-iS_{\text{st}}(t, \tau)] \right\} \quad (2)$$

within the stationary phase approximation, which leads to the stationary action

$$S_{\text{st}}(t, \tau) = \tau |E_0| - \frac{\tau}{2} p_{\text{st}}^2(t, \tau) + \frac{1}{2} \int_{t-\tau}^t dt' A^2(t'), \quad (3)$$

while the stationary momentum is given by

$$p_{\text{st}}(t, \tau) = \frac{\mathcal{E}_0}{\omega_L \tau} [\sin(\omega_L t) - \sin(\omega_L t - \omega_L \tau)]. \quad (4)$$

Thus, in Eq. (2) the dipole at time  $t$  receives contributions from all trajectories that started at the origin a time  $\tau$  earlier, picked up the action  $S_{\text{st}}$ , and returned to the origin at  $t$ , which for a free classical evolution is possible only for a definite average momentum,  $p_{\text{st}}$ . The quantity  $d_x(p)$  represents the interaction with the bound state and is usually taken as some approximation to the dipole matrix element between the ground state and the continuum state at energy  $E_p = p^2/2$ .

In order to compute the wavelet transform of the dipole acceleration from  $x(t)$ , one must use the formula

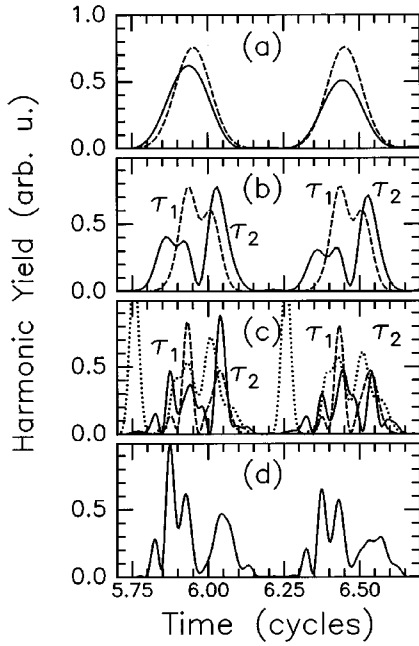


FIG. 1. Wavelet analysis of the time-dependent dipole acceleration over one cycle of the driving laser field. (a)  $N=49$ ,  $\sigma=0.1$  T; (b)  $N=45$ ,  $\tau=0.055$  T; (c), (d)  $N=37$ ,  $\tau=0.024$  T. Solid line: full time-dependent solution; dashed line: two-step model [1,4] with Gaussian dipole approximation, dotted line [only in (c)]: two-step model with exact dipole. The solid line in (d) is for a projection of the fully time-dependent dipole onto the unperturbed bound state.

$$\int dt \ddot{x}(t)W(t) = - \int dt x(t)\ddot{W}(t), \quad (5)$$

where the function  $W(t)$  is in our case the analyzing wavelet  $W(t, t_0, \Omega)$  with second derivative  $\{(-2/\sigma^2) + [i\Omega - 2(t-t_0)/\sigma^2]^2\}W(t, t_0, \Omega)$ . This is obtained by partial integration, noting that  $W$  and its derivatives vanish at the integration endpoints.

Figure 1 presents the results from the time-frequency analysis over one cycle; we show the square of the magnitude of the quantity (5) for  $t_0$  varying from 5.7 to 6.7 T. The dashed lines in the figure correspond to the results obtained using the two-step model [1], while the solid lines are the results of the full time-dependent solution.

Peaks in the harmonic time-frequency spectrum arise from classical trajectories returning to the origin, leading to strong nonlinear response within the range of the potential. These classical return time peaks are clearly visible in the harmonic response centered on the cutoff harmonics ( $\Omega=49 \omega_L$ ,  $\sigma=0.1$  T), for both the fully time-dependent and the semiclassical calculation, shown in part (a). This has been observed before in [3]. When more plateau harmonics are included, as in Fig. 1(b), ( $\Omega=45 \omega_L$ ,  $\sigma=0.055$  T) the single peak splits into two, whose temporal positions correspond approximately to the two (semi) classical shortest return times,  $\tau_1$  and  $\tau_2$  (see Fig. 3 in [4]). It is, however, apparent that the two peaks are farther apart for the full solution than for the two-step model. Furthermore, the  $\tau_1$  peak has gained additional substructure in the full solution.

When most of the plateau harmonics are included, in Fig. 1(c), there are still two dominant peaks; the “shortest clas-

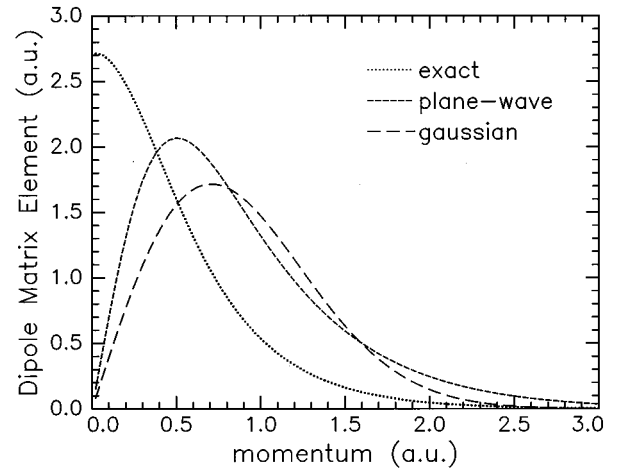


FIG. 2. Dipole matrix elements  $d_x(p)$ . Dotted line: exact; dashed line: plane-wave continuum approximation; short-dashed line: “Gaussian” approximation.

sical return” peak (denoted by  $\tau_1$ ) is composed of many subpeaks since many harmonics are included. In fact, the shorter return time varies more rapidly with harmonic energy. The return peak  $\tau_2$  is prominent in both sets of results. This is comparable to the case considered in [4], Fig. 2.

Our results show that the semiclassical model contains the essential physics leading to high-harmonic generation in a linearly polarized laser field. The multiple peak structure of [4] is reproduced in qualitatively similar fashion in both results, with peaks at similar positions and of similar magnitude.

However, the agreement is good only for a special choice of the “atomic dipole” function  $d_x(p)$ , namely,  $d_x(p) \sim p e^{-\alpha p^2}$ , with  $\alpha=1$ , shown as the short-dashed line in Fig. 2. This “Gaussian dipole” approximation to the dipole matrix element corresponds to a Gaussian ground-state wave function in position-space and plane-wave continuum wave functions. If we take for  $d_x(p)$  the exact dipole matrix element between the bound state and the continuum state at energy  $p^2/2$  (given as the dotted line in Fig. 2) we obtain the dotted line in Fig. 1(c), exhibiting a strong spurious peak near  $\mathcal{E}=\mathcal{E}_0$ . This spurious peak appears generally in the stationary phase approximation when the width (in  $p$  space) of  $d_x(p)$  is made so small that the contribution near the “zero-time” trajectory is strongly peaked: physically this would correspond to contributions near the origin from parts of the wave function that are being “accelerated” by the field within the range of the potential. It is evident from the full time-dependent solution (solid line) that this is not an important mechanism of harmonic generation in the present case. Furthermore, for such a peaked  $d_x(p)$ , the stationary phase approximation starts to become invalid.

In the actual physical process of high-harmonic generation at low laser frequency the “rescattering” wave packet appears through a tunnel ionization process and thus it is not astonishing that the modeling through a dipole matrix element is not adequate. On the other hand, for the second interaction in Eq. (2), which “generates the harmonics,” the dipole matrix element should be quite appropriate.

Finally, in Fig. 1(d) we consider the time-dependent dipole including the projection [6] onto the bound state  $|0\rangle$ , namely,  $x_0(t) = \langle \psi(t)|0\rangle\langle 0|x|\psi(t)\rangle$  [7]. This projection retains only contributions from bound-to-continuum dipole “transitions.” Although the harmonic spectrum resulting from this projection is very close to the harmonic spectrum from the full solution, the time dependence [using Eq. (5)] shown in Fig. 1(d) is different from the exact one [solid line in Fig. 1(c)], being closer to the one from the “Gaussian dipole” two-step model [dashed line in Fig. 1(c)], in particular with respect to the broader  $\tau_2$  peak and the minima at  $t=5.97$  and  $6.47$ . For the group of  $\tau_1$  peaks, the same peaks are observed, but the ones corresponding to earlier return times appear strongly suppressed in the two-step model. It thus appears that the “continuum-to-continuum transitions” play an important though not decisive role in explaining the difference between the full solution and the two-step model [8].

It must be noted that in our one-dimensional case the transverse spreading of the wave packet is not present and thus the higher-order returns to the origin at later times tend to be enhanced in probability [we have an exponent  $1/2$  instead of the usual  $3/2$  in Eq. (2)]. In both models effects of propagation and phase matching [4] were not included. Our time profile from the full solution is only approximately symmetric under a shift of  $0.5 T$ . This is clear since in our fully time-dependent case there is strong ionization and thus the dipole moment decays in time, in addition to other explicitly time-dependent effects. Finally, although we are probing the harmonic response over times shorter than the laser field period, the harmonic generation process must happen over several cycles of the laser field in a quasiperiodic fashion [9].

Obviously, the Fourier transform of any harmonic comb frequency spectrum leads to a temporally peaked time spectrum, but only the particular phases inherent to harmonic generation will lead to the present peak distribution. Con-

cluding, the general plateau harmonic generation spectra are reproduced by a wide variety of models. The classical return cutoff [5] is reproduced by all models including a “quasifree” returning electron. But the time dependence of the harmonic generation is a much more differential and thus sensitive measure, in which not simply the magnitudes but the relative phases of all contributing harmonics are involved. When only cutoff harmonics are involved, as shown in Fig. 1(a), the time of harmonic generation is just  $0.45$  and  $0.95$  in units of the laser period, that is, just before the peak of the field. This result again is not very sensitive: most models correctly predict the phase of the *cutoff* harmonics. However, when more and more of the *plateau* harmonics are superposed, a much more complex time behavior emerges. From the full time-dependent solution, it is clear that the semiclassical picture that predicts two dominant shortest return time peaks is qualitatively correct, as shown by the solid line with the peaks  $\tau_1$  and  $\tau_2$  in Figs. 1(b) and 1(c). The exact shapes and substructure of these peaks are, however, not quantitatively reproduced by the two-step model. First, we found that a spurious peak can appear at  $\mathcal{E}(t) = \mathcal{E}_0$  when  $d_x(p)$  is chosen too peaked in the two-step model. Second, the shortest return time  $\tau_1$  peak splits into several peaks with comparable magnitude. The two-step model indicates that one of these is dominant, which is not the case in the full solution. Third, the longer return time  $\tau_2$  peak is narrower in the full solution. A projection  $x_0(t)$  involving only continuum-to-bound transitions from the full time-dependent solution leads for the  $\tau_2$  peak to closer agreement with the two-step model. This  $\tau_2$  peak appears stably isolated in all three cases and should thus be a better candidate for propagative selection [4] than the strongly model-dependent series of  $\tau_1$  peaks.

C.F.M.F. was supported by the DAAD and M.D. was supported by the Deutsche Forschungs-Gemeinschaft. C.F.M.F. is grateful to A. Fring and to A. Lohr for useful discussions.

- 
- [1] M. Lewenstein, Ph. Balcou, M. Yu. Ivanov, A. L’Huillier, and P. B. Corkum, *Phys. Rev. A* **49**, 2117 (1994).
- [2] See, e.g., K. Burnett, V. C. Reed, J. Cooper, and P. L. Knight, *Phys. Rev. A* **45**, 3347 (1992); J. L. Krause, K. Schafer, and K. Kulander, *ibid.* **45**, 4998 (1992).
- [3] S. C. Rae, K. Burnett, and J. Cooper, *Phys. Rev. A* **50**, 3438 (1994); P. Antoine, B. Piraux, and A. Maquet, *ibid.* **51**, R1750 (1995); R. Taieb, A. Maquet, P. Antoine, and B. Piraux, in *Proceedings of the Super-Intense Laser-Atom Physics IV Conference*, edited by H.G. Muller and M. V. Fedorov (Kluwer, Dordrecht, 1996); P. Antoine, B. Piraux, D. B. Milosevic, and M. Gajda, *Phys. Rev. A* **54**, R1761 (1996).
- [4] P. Antoine, A. L’Huillier, and M. Lewenstein, *Phys. Rev. Lett.* **77**, 1234 (1996).
- [5] The peak excursion amplitude in our case is  $\alpha_0 = \mathcal{E}_0/\omega^2 = 32$  a.u. The plateau extends to roughly the photon energy  $E_c = E_0 + 3E_p$ , with the ponderomotive energy  $E_p = \mathcal{E}_0^2/4\omega_L^2$  a.u. In the present case the cutoff energy is at  $E_c = 49\omega_L$ .
- [6] J. B. Watson, A. Sanpera, and K. Burnett, *Phys. Rev. A* **51**, 1458 (1995).
- [7] We have used the equality  $\langle \psi(t)|\dot{x}|\psi(t)\rangle = \langle \psi(t)|-dV(x)/dx + \mathcal{E}(t)|\psi(t)\rangle$  to compute  $\dot{x}(t)$ , as discussed in [2]. This equality cannot be used [6] for computing the quantity  $\ddot{x}_0(t) = \langle \psi(t)|0\rangle\langle 0|\ddot{x}|\psi(t)\rangle$ , since Ehrenfest’s theorem (from which the equality above follows) holds only for expectation values and not for the “transition” matrix elements  $x_0(t)$ . Stated otherwise, the projection operator  $|0\rangle\langle 0|$  does not commute with the full Hamiltonian  $H(t) = p^2/2 + V(x) + p \cdot A(t)$ .
- [8] The comparison of the two-step model and the delta-potential Floquet solution [W. Becker, S. Long, and J. K. McIver, *Phys. Rev. A* **41**, 4112 (1990); **50**, 1540 (1994)] concerning in particular continuum-continuum transitions is addressed by W. Becker, A. Lohr, M. Kleber, and M. Lewenstein, *Phys. Rev. A* (to be published).
- [9] See, e.g., M. Protopapas, D. G. Lappas, C. H. Keitel, and P. L. Knight, *Phys. Rev. A* **53**, R2933 (1996).
- [10] K. J. Schafer and K. J. Kulander, *Phys. Rev. Lett.* **78**, 638 (1997), have also performed a time-frequency analysis of cutoff harmonics, for ultrashort pulses.